FMBEM analysis of sound scattering from a damping plate in the near field of a hydrophone

Daniel Wilkes[1], Polly Alexander[2 3], and Alec Duncan[1]

[1]CMST Curtin University, Kent Street, Bentley, Perth, WA, 6102, Australia
[2]Australian Maritime College, UTAS, Maritime Way, Launceston, TAS 7248, Australia
[3]Intelligent Sensing and Systems Laboratory, CSIRO ICT Centre, Hobart, TAS, 7000, Australia

ABSTRACT

As part of research into the effect of underwater noise on the communication between an under-ice Autonomous Underwater Vehicle (AUV) and it's stationary launch vessel (the Aurora Australis), fast multipole boundary element method (FMBEM) acoustic modeling was conducted. In particular, a steel damping plate with a complex 3-dimensional structure was modeled (using up to 1.6 x 10^5 boundary elements) and the effect of sound scattering from a pinger near the ship was determined at the receiver hydrophone, which was in close proximity to the damping plate. The direct incident field from the pinger was modeled as a plane wave at a number of incidence angles (to account for the depths to which the hydrophone was lowered) and over a range of frequencies up to the pinger frequency of 10kHz. This paper presents these results and discusses some of the interesting effects observed at the 'non-unique' frequencies when using the different methods available to provide stability to the numerical solution. Thus far, the modeling conducted for the damping plate has treated the object as rigid. The FMBEM code being developed at CMST now has the capability to model fully coupled fluid-structure interactions and some initial results from treating the damping plate as elastic are also presented.

INTRODUCTION

Polar under ice Autonomous Underwater Vehicle (AUV) deployment is a high risk operation. This is due to the remoteness of the experiment location, the limitations the ice cover places on AUV emergency surfacing strategy and the effects of the ice canopy on underwater communications. In ship based operations the ship acts as a listening station for status and emergency signals from the AUV during a mission. The use of this ship as a listening station means that the communication channel is further compromised by the interference of ship noise. To determine the effects of using the Australian Antarctic Division's vessel the *Aurora Australis* as an AUV deployment platform a series of noise experiments were carried out on location in the sea ice in 2010.

The recording setup for these experiments consisted of an omni directional hydrophone lowered to depths of as much as 380m below the ship with noise recordings made at different depths. A calibrated 10kHz sound source was used to simulate the ship noise at the upper limit of the full ship noise range (1-10kHz). During this experiment the hydrophone was placed somewhere between 4 and 20cm below a steel damping plate and weighting structure, used to stabilise the hydrophone.

One aspect of the experimental error analysis investigated was to determine what effect near field scattering from the damping plate had in the local region where the hydrophone was hung from the plate. This was achieved by numerically modeling the scattered acoustic field from the plate using a fast multipole boundary element method (FMBEM). The sound source was modeled as a 10kHz plane wave at different incidence angles corresponding to the various hydrophone depths and the calculated total acoustic field in the region of interest was compared to the incident field (i.e. the field in the absence of the structure) at the same points to determine a relative error bound due to near field scattering from the plate into the receiver. The numerical modeling was then extended to include a number of frequencies over the ship noise profile and different orientations, to observe the variation in the near field as the damping plate was rotated about the vertical axis.

The FMBEM is essentially the amalgamation of two methods: the boundary element method (BEM), which is the numerical implementation of the governing boundary integral equation (BIE) for the problem being solved (Wrobel 2002), and the fast multipole method (FMM), which provides a substantial reduction in the algorithmic complexity and memory requirements of the BEM (Coifman, Rokhlin, and Wandzura 1993). The BEM is a common choice for modeling fluid regions exterior to a finite object as the problem must only be solved on the boundary surface and there is no computational penalty associated with modeling infinite domains (Jensen et al. 2000). This method is implemented by discretising the surface into a number of elements, forming a system of equations relating the boundary integral at each of these elements and simultaneously solving the resulting matrix equation at each element with appropriate boundary conditions. The BEM may also be used to model a problem interior to a boundary surface (again restricting all unknowns to the surface), but a more common choice is the finite element method, which allows material properties to vary per element (Chen 2005) at the expense of discretising the entire enclosed volume of interest (Zienkiewicz and Taylor 2000).

The main disadvantages of the BEM are that the coefficient matrices resulting from the surface discretisation are dense, complex and non-symmetric (Xiao and Chen 2007), as apposed to the sparse, real and banded matrices resulting from the finite element method (Reddy 2004) and that the method yields non-unique solutions for the exterior problem at certain frequencies (Kirkup 1998). This non-uniqueness is a result of the numerical discretisation of the boundary surface into a coefficient matrix (describing the interaction between each and every pair of elements) which will be singular for certain eigenfrequencies and this has been shown to be the case for all of the possible acoustic boundary conditions (Neumann, Dirichlet and Robin) (Wu 2000). These characteristic frequencies always correspond to those for the interior Dirichlet problem (Marburg and Wu 2008), where they have a physical significance for the interior enclosed boundary surface. Common solution methods applied to the exterior BEM to ensure a unique solution at all frequencies are the CHIEF method, which includes additional zero-pressure points inside the surface (Schenck 1968) and solves the resulting over-determined system of equations (Amini, Harris, and Wilton 1992), and the Burton-Miller formulation, which solves a combined system of 2 BIEs involving a complex-valued coupling parameter (Burton and Miller 1971).

The BEM modeling of the damping plate was conducted with the FMBEM code being developed at CMST as well as a standard BEM model from a commercial numerical software package. Initially the Burton-Miller formulation was used as the stabilisation method in both the numerical models and was observed to have a significant effect on the calculated pressure over certain parts of the model. However the agreement of the calculated results between the models was not entirely convincing. The commercial software could alternatively use the CHIEF method in the BEM solution and again it was observed that the agreement between the FMBEM/BEM models at the suspected eigenfrequencies was poor. Furthermore, the calculated total surface pressure for the damping plate between the 2 BEM models from the commercial software package also displayed discrepancies, with the only difference being the stabilisation technique used. These results indicated that the numerical solutions of the model were sensitive to the solution method used and it was surmised that this might be due to the particular shape of the damping plate and the fact the model was being treated as rigid (which may not be a valid assumption over the frequency range of interest).

This paper presents and discusses the FMBEM and BEM results of the damping plate yielded by the non-uniqueness mitigation techniques mentioned above. The initial sections of this paper discuss the set-up of the noise experiment with reference to the numerical modeling and briefly review the background theory for the BEM and FMBEM acoustic modeling. The next sections discuss the rigid numerical modeling and the initial fully coupled modeling respectively. Finally, some conclusions are presented.

THE EXPERIMENT

A photo of the hydrophone deployment setup is shown in Figure 1. The yellow object is the steel damping plate and weight structure that was numerically modeled. The structure can be broken into the top disk, a cylindrical open-ended tube, a fin, and two angle brackets. The top disk has a 2cm radial cut stopping just short of the

Figure 1: A photo of the hydrophone (black cylindrical shape) attached ready for deployment to the steel weight and damping structure (yellow).

tube where the hydrophone cable is being fed through. The distance that the hydrophone was positioned below the end of the tube was not measured and is likely to have changed between different experimental runs. To account for this the analysis was undertaken within a 15cm x 15cm x 16cm cubic field starting 6cm below the bottom of the structure. This bounding box should also take into effect swing of the hydrophone with current away from the direct axis of the structure. The orientation of the structure in the water column with respect to the incident field was also unknown, as the damping plate may have twisted about the cable. To consider the effect of this uncertainty the numerical analysis was undertaken at a range of orientation angles about the plane of symmetry of the damping plate.

The calibrated sound source used in the experiment was a RJE model no ULB-364/10-PL wet activated 10 kHz beacon with a listed output of 183 dB re 1uPa at 1m. It has 5 ms pulse length and 42 second period between pulses. The beacon was deployed at approximately 10.5m depth and the horizontal displacement between the beacon and the hydrophone was calculated to be 11m. The hydrophone system was lowered from the aft deck to depths down to 380m. This created a changing angle of incidence of the sound field from the beacon between 48 degrees above and 90 degrees below the horizontal. For the noise profile experiment the far field measurements were of greater interest and so the analysis was undertaken for an incidence angle range of 15 to 88 degrees below the horizontal.

BEM/FMBEM ACOUSTIC MODELLING

The governing equation of interest for acoustic modeling using either BEM is the integral form of the Helmholtz differential equation (Mechel 2008). For an infinite exterior fluid domain containing an acoustic source impinging an incident acoustic field p^{inc} on a boundary surface S, the Helmholtz BIE is:

$$-\frac{1}{2}p(\mathbf{y}) = \int_S \left[\frac{\partial G(\mathbf{x},\mathbf{y})}{\partial \mathbf{n}(\mathbf{x})} p(\mathbf{x}) - G(\mathbf{x},\mathbf{y}) \frac{\partial p(\mathbf{x})}{\partial \mathbf{n}(\mathbf{x})} \right] dS(\mathbf{x}) \\ - p^{inc}(\mathbf{x}) \tag{1}$$

where p and $\frac{\partial p(\mathbf{x})}{\partial \mathbf{n}(\mathbf{x})}$ are the total pressure and its outward pointing normal derivative, $\mathbf{x}$ and $\mathbf{y}$ are points on S (assumed to be locally smooth at $\mathbf{y}$) and $G(\mathbf{x},\mathbf{y})$ is the Helmholtz fundamental solution or free-space Green's function (Gaul, Brunner, and Junge 2009). $G(\mathbf{x},\mathbf{y})$ takes the form of a spherically radiating point source:

$$G(\mathbf{x},\mathbf{y}) = \frac{e^{ikr}}{4\pi r} \tag{2}$$

where r is the magnitude of the distance between $\mathbf{x}$ and $\mathbf{y}$, k is the wavenumber and i is the complex number (Liu 2009). The effects of sound absorption can be incorporated into equation (1) by making the wavenumber a complex value (Ihlenburg 2008).

The Burton-Miller formulation provides a unique solution to the Helmholtz BIE at all frequencies by combining equation (1) with the normal derivative of the equation applied at $\mathbf{y}$ (Li and Huang 2010). The coupling parameter between the 2 BIEs must be complex to yield a unique solution at all frequencies (Liu and Rizzo 1992) and is usually made inversely proportional to the wavenumber. Conversely, the CHIEF method provides stability to the Helmholtz BIE by introducing additional equations which set the total pressure to zero at arbitrarily chosen points inside the boundary surface (Amini, Harris, and Wilton 1992). Unfortunately, CHIEF points placed at locations already corresponding to zero pressure points for the equivalent interior problem do not stabilise the BIE (Hwang 1997) and these points are generally not known *a priori*. However it has been shown that only one non-zero CHIEF point is required to obtain a unique solution (Seybert and Rengarajan 1987).

Numerical solution of equation (1) is achieved by discretising the surface into a number of elements and posing the equation with respect to each element. The surface integrals are implemented as a sum of numerical integrals (i.e. via Gaussian quadrature or a similar technique) over the elements which approximate the surface. Application of the boundary conditions will eliminate one of the unknowns (p or q) on the right hand side of equation (1) yielding a system with as many equations as unknowns. The BEM may solve this system of N unknowns directly for a cost of N^3 operations or iteratively for a cost of N^2 operations per iteration (Gumerov and Duraiswami 2009). These algorithmic complexities come about from the fact that the pressure at any point on the boundary is dependent on the pressure at every other point due to the surface integrals in the Helmholtz BIE. When discretised, the interactions are between each pair of boundary points and are described by the Green's function in equation (2). Thus the standard BEM constructs and stores the Green's function coefficient matrix which require the order of N^2 memory to store and N^2 operations for each iterative multiplication – a prohibitive cost for large problems

The FMBEM reduces both the algorithmic complexity and memory requirements of the BEM by approximately calculating the product of the matrix-vector multiplication without explicitly forming the coefficient matrix and by dealing with interactions between groups of boundary elements (Amini and Profit 2003). The key mechanism of the FMBEM is to separate the Green's function into a pair of independently calculable series expansions which introduce an intermediate point or expansion centre between the boundary points $\mathbf{x}$ and $\mathbf{y}$ (Brunner et al. 2010). A number of different types of series expansions have been investigated for the Helmholtz equation, broadly catagorised into high and low frequency expansions (in reference to the frequency regimes in which the expansions are used) (Nishimura 2002). One possible choice is the Singular S and Regular R spherical basis functions:

$$S_n^m(\mathbf{r}) = j_n(kr)Y_n^m(\theta,\phi) \qquad (3)$$
$$R_n^m(\mathbf{r}) = h_n(kr)Y_n^m(\theta,\phi) \qquad (4)$$

where $n = 0, 1, 2...$ and $m = -n : n$ are the degree and order of the expansion, j and h are the spherical Bessel and Hankel functions

of the first kind and $Y_n^m(\theta,\phi)$ is the spherical harmonic function (Gumerov and Duraiswami 2003). Equations (3) and (4) may be combined to build the Helmholtz Green's function between points $\mathbf{x}$ and $\mathbf{y}$ as follows:

$$G(\mathbf{y} - \mathbf{x}) = ik \sum_{n=0}^{\infty} \sum_{m=-n}^{n} R_n^{-m}(\mathbf{x} - \mathbf{c})S_n^m(\mathbf{y} - \mathbf{c}) \qquad (5)$$

valid for $|\mathbf{x} - \mathbf{c}| < |\mathbf{y} - \mathbf{c}|$ (Gumerov and Duraiswami 2004). Series expansions centred about similar expansion points may be combined into single sets of coefficients and thus interactions between 'well separated' groups of elements may be considered in the FMBEM. Furthermore, the expansion centres may be shifted with appropriate translation algorithms allowing the domain of validity of the expansions to be varied and so the expansions of local groups of elements may be re-used. Thus the surface integrals required to calculate the pressure at each point on the boundary surface may be split into a far region, where the well separated criterion is met and the FMM may be used, and a near region, where the integrals are directly calculated and stored as with the BEM (Gumerov and Duraiswami 2007).

RIGID DAMPING PLATE ANALYSIS

The initial analysis of the damping plate involved the construction of two boundary meshes, shown in Figure 2, being a high resolution FMBEM model containing 166,326 plane triangular elements (each with one pressure degree of freedom (DOF)) and a lower resolution BEM model containing 8,196 elements/DOFs (corresponding to approximately 44 and 9 elements/λ respectively at 10kHz). The FMBEM model was constructed in part to test the FMBEM code on larger scale problems to ascertain the capabilities of the code and also to determine if a much coarser model (with some of the fine detail of the plate removed) could be used in the analysis without significantly changing the results. The main differences are that the low resolution model does not include the rebar loop for hanging the damping plate or the lip on the edge of the circular plate, the end of the cut-out in the circular plate is approximated as a square cut instead of a semi-circle cut and the attachment of L-shaped plates is simplified to a continuous connection. The results shown in Figure 2 are the calculated total surface pressure from a 10kHz incident plane wave traveling at 45 degrees below the horizontal and in the plane of symmetry of the model. This orientation of the incident field with respect to the plate is used for the remainder of the paper for comparisons with the commercial software.

Obviously as the mesh discretisations are different a direct comparison of the calculated total surface fields cannot be made for the two meshes shown Figure 2. However, the off-surface received field (calculated from the total surface pressure) in the cubic region encapsulating the hydrophone were calculated on exactly the same grids. These sets of results had a relative residual norm of 4.4% for the entire set of received field planes, indicating that the low resolution damping plate gives a good approximation to the damping plate with significantly fewer unknowns. Furthermore the mesh has enough elements to satisfy the usually quoted 'X nodes per wavelength' rules, where X is a small integer typically less than 10 (see for example (Marburg 2008)) up to the maximum 10kHz frequency. Thus the low resolution mesh was used for the numerical modeling over the full range of frequencies and incident angles.
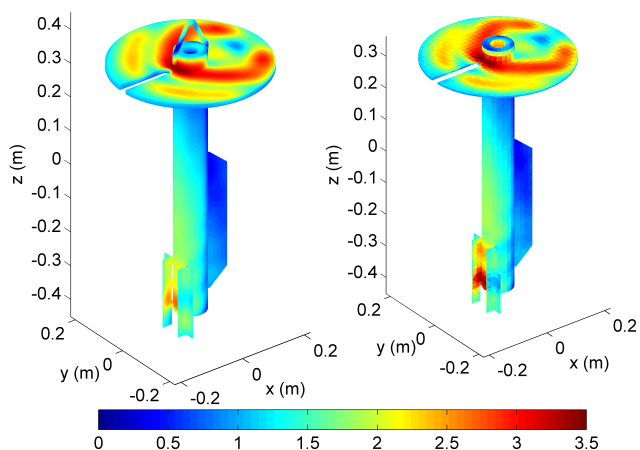
Figure 2: Comparison of high resolution (left) and low resolution (right) damping plate models. The colour variation indicates the total surface pressure in Pascals for a 10kHz unit strength incident plane wave.

The commercial software was able to use either the Burton-Miller or CHIEF methods to stabilise the Helmholtz BIE and so both methods were used to compare to the FMBEM results at one incident field orientation at each of the frequencies ranging from 0.5-10kHz in 0.5kHz increments. The times to set up and solve the total surface pressure at 1kHz for the commercial software were 38.3 minutes and 36.8 minutes using the Burton-Miller and CHIEF methods respectively. The FMBEM software solved the same problem in 151 seconds but the convergence of the iterative solver slowed down as the frequency increased (as apposed to the solution time of the BEM software which seemed to be independent of the frequency), solving in about 380 seconds at 10kHz. The FMBEM code solved the high resolution mesh at 10kHz (pictured left in Figure 2) in 5.2 hours, with 260 iterations required to reach the 10^{-4} convergence criterion. This slow convergence can be attributed to the damping plate model around the connection of the rebar loop and the cylinder, where the boundary element surfaces are very close together and facing each other. Although appropriate methods are used to deal with near-singular and singular integrals in the near field of each element, it appears (at least for the rigid boundary condition) that the solution for constant pressure triangular elements in these regions is quite unstable. Re-running the model with the loop removed (which reduced the number of elements to 155,843) almost halved the number of iterations to 131 for a similar convergence criterion. The BEM software was unable to solve the high resolution mesh: the coefficient matrix would require a few hundred Gb of space to store and the computation time to apply even one matrix-vector product to such a volume of data would be prohibitively large.

A plot of the relative residual norms between the FMBEM and two BEM results for the low resolution plate is shown in Figure 3. This plot also shows the relative residual norms between the sets of BEM results, where the only difference in the solution process is the method used (CHIEF, Burton-Miller) for providing numerical stability to the BIE.

The plot of the relative residual norms (which represent a measure of the disagreement or 'error' between the numerical models) between the FMBEM and BEM solutions in Figure 3 shows several interesting features: the most obvious being the error spikes at 1kHz
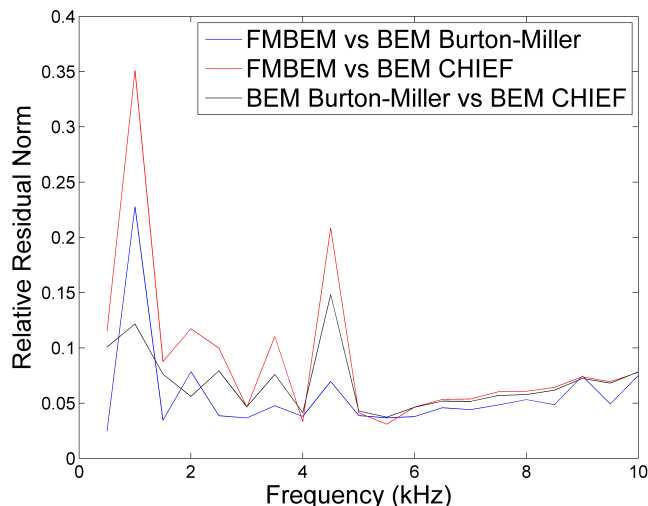
Figure 3: Plot of the relative residual norms versus Frequency between the FMBEM and commercial software results for the total surface pressure on the damping plate.

and 4.5kHz. At 1kHz it can be seen that the higher errors are from the comparison of the FMBEM and BEM results (although the error between the two sets of BEM results is still about 12%), which indicates that there may be an issue with the FMBEM solution. The well-separated part of the surface field, calculated via the FMM, of 400 randomly chosen surface elements was compared to the same field yielded from applying a 5×5 Gaussian quadrature rule. The relative residual norm between these results (which in this case may be considered as the error involved with treating the well-separated part of the field with the FMBEM instead of the BEM) was only 0.58%. The FMBEM solution was re-calculated with a larger seperation distance (i.e. with more of the field treated with the BEM and less with the FMBEM) and the relative residual norm with the Burton-Miller and CHIEF BEM solutions reduced to 5.47% and 16.81% respectively. This indicates that the calculated total surface pressure at 1kHz was sensitive to the errors introduced by the FMBEM but the large errors that still exist between the Burton-Miller and CHIEF results suggest that there also is another factor involved. Similarly, the spikes in the errors at 4.5kHz are due to the poor agreement of the Burton-Miller and CHIEF results.

The above discussion of the relative residual norms between the solutions at 1kHz and 4.5kHz suggests that there is poor agreement between the Burton-Miller (BEM or FMBEM) and CHIEF methods. The most common technique used to determine the stability of the numerical solutions is to change the complex coupling parameter between the BIEs of the Burton-Miller formulation or to vary the number of CHIEF points for the CHIEF method. In either case, varying these parameters should not change the solution substantially for a well-conditioned problem. Focusing on the 1kHz results it was observed that halving the Burton-Miller parameter varied the results by 2.2% while doubling the number of CHIEF points appeared to have no effect on the solution calculated by the commercial software, indicating that the solutions at 1kHz were fairly stable. The main discrepancies between the two total surface pressure fields are occuring along the inner cylinder surface. In fact, a similar comparison of the surface field excluding the the inner surface of the cylinder reduces the relative residual norm between the FMBEM and CHIEF BEM results to 2.4% (compared to 35% for the

full field), indicating that the error between the solutions is localised to the inner cylinder surface. The field on the inner cylinder (Figure 4) shows the total surface pressure calculated by the FMBEM and CHIEF BEM for half of the model cut along the plane of symmetry.
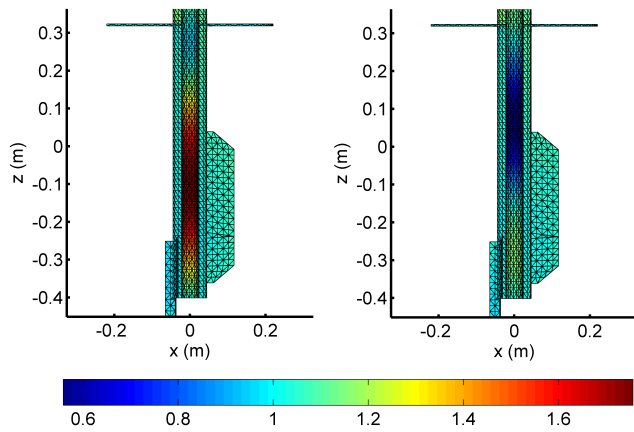
Figure 4: Comparison of the FMBEM (left) and CHIEF BEM (right) calculated total surface pressure for a 1kHz unit strength incident plane wave shown in the plane of symmetry for the low resolution damping plate model. The colour variation indicates the total surface pressure in Pascals.

Figure 4 shows that the FMBEM code has calculated a peak in pressure near the centre of the cylinder but shifted away from the end with the cylindrical plate while the CHIEF method has predicted a low pressure point shifted in the opposite direction. The main part of the damping plate structure is an open-ended cylinder and so the model should exhibit resonances close to the frequencies corresponding to standing waves inside the cylinder (particularly at the lowest node there should be a peak in pressure in the middle of the cylinder). Perhaps the most appropriate end corrections for the resonant frequency formula are to approximate the end of the cylinder with the circular plate as flanged (using half of the flanged pipe end correction 0.8217 (Nomura, Yamamura, and Inawashiro 1960)) and the other end as open (using half of the open pipe correction 0.6133 (Silva et al. 2009)), giving the frequencies f as:

$$f = \frac{pv}{2L + d(0.4108 + 0.3066)} \qquad (6)$$

where L is the cylinder length, d is the inner diameter and p is an integer for the pth mode. This formula gives the resonant frequencies of the pipe section of the damping plate as integer multiples of 866Hz. Therefore the first mode may be contributing to the error at 1kHz but it would suggest that a strong resonance and most likely a proportional disagreement between the Burton-Miller and CHIEF methods should occur at 3.5kHz (being within 40Hz of the forth mode). While there is some increase in the error between the methods at 3.5kHz, the peak in the errors occur at 4.5kHz which would be almost 170Hz from the 5th mode: a moderate difference. A similar plot of the total surface pressure at 4.5kHz from the FMBEM and CHIEF BEM methods along the plane of symmetry of the damping plate is shown in Figure 5.

It can be seen from Figure 5 that the total pressure field at 4.5kHz must be close to the 5th mode of the cylindrical part of the damping plate. A more accurate measure of the resonant frequency can be
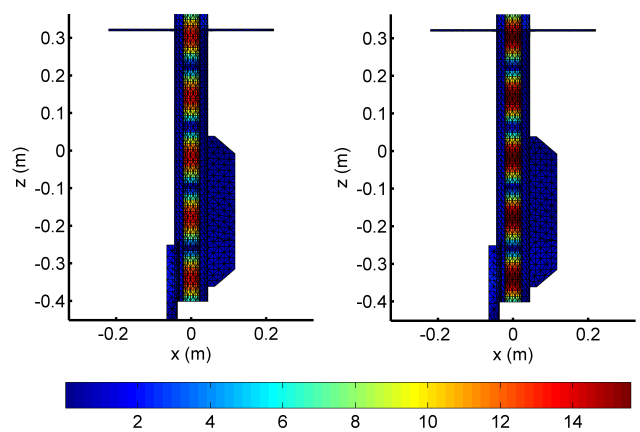
Figure 5: Comparison of the FMBEM (left) and CHIEF BEM (right) calculated total surface pressure for a 4.5kHz unit strength incident plane wave shown in the plane of symmetry for the low resolution damping plate model. The colour variation indicates the total surface pressure in Pascals.

determined by calculating the total surface pressure over a range of frequencies and looking for a peak in the pressure amplitude. This was done using the commercial software's Burton-Miller formulation and by refining the frequency around 4.5kHz, giving the plot of peak total pressure versus frequency shown in Figure 6.
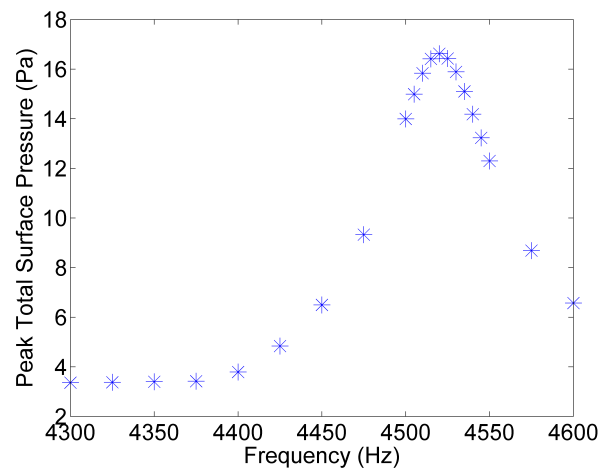
Figure 6: Plot of the peak total surface pressure versus frequency for the low resolution damping plate. The incident field again had an amplitude of 1 and was directed 45 degrees below the x-axis in the xz-plane.

The peak pressure calculated by the model around the 5th mode was at 4520Hz and so the exact frequency of this mode must lie within $\pm$5Hz (the increments used around this frequency). This gives the modal frequencies of the damping plate as integer multiples of 904$\pm$1Hz, which would explain the large error observed between the numerical models at 4.5kHz in Figure 3. The smaller error peak at 3.5kHz lies within 100Hz of the 4th mode and so the error between the numerical models may be due to the differences in the peak pressure calculated by the Burton-Miller and CHIEF methods near that frequency (Figure 6 shows the extent of the increased peak pressure is about $\pm$100Hz from the resonant frequency). A similar argument can be put forward for the model errors at 1kHz, al-

though it has already been established from Figure 4 that the CHIEF method calculated a pressure low at 1kHz where as an open ended pipe should have a pressure peak at the lowest mode (as was calculated by the FMBEM and BEM Burton-Miller methods). The error peak at 2kHz appears to be outside the range of effect of the peak pressure discrepancies between the Burton-Miller and CHIEF methods. The larger errors at 2kHz are between the FMBEM and BEM methods which again implies that the disagreement between the models is due in part to the approximations introduced by the FMBEM (as was the case at the 1kHz results). It is likely that the errors between the model results at 2kHz are due to a combination of these factors, as was the case at 1kHz.

DAMPING PLATE ANALYSIS WITH COUPLED FLUID-STRUCTURE INTERACTION

Thus far the analysis of the damping plate has treated the object as rigid, allowing the problem to be fully described by the Helmholtz BIE. A more realistic analysis of the problem is to treat the solid as elastic and allow the acoustic field to distort the structure, which in turn affects the scattered field, i.e. a coupled fluid-structure interaction. Therefore an interior model of the structure is also required and this usually takes the form of a finite element method, due to the favorable properties of this method for modeling finite domains (as discussed in the introduction). The infinite exterior fluid region is treated in a similar manner as the rigid acoustic model (i.e with the same Helmholtz BIE) and the two models are coupled on the shared boundary surface to give the interaction between the fluid and structure (Ali and Rajakumar 2004). Boundary conditions can be enforced on the shared surface to reduce the number of unknowns to two (the surface displacement and the total surface pressure) and the coupled system of equations simultaneously solved for both unknowns.

Of course the disadvantages cited for the BEM still stand when using the method in a coupled analysis. An obvious step in improving the model would be to use the FMBEM to model the exterior acoustic region and couple this to an interior FEM model. Such models have been developed (Fischer and Gaul 2005) and various aspects, particularly of the coupling between non-conformant meshes (where lower resolutions are required in the structure due to the significantly higher sound speeds of common building materials i.e. steel, compared to that for the fluid), have been investigated by several authors (Schneider 2008, Gaul, Brunner, and Junge 2009, Brunner, Junge, and Gaul 2009). For simple interior structures like solid objects or those involving a few regions of piece-wise constant material properties, it may be advantageous to treat the interior solid domain with a BIE which restricts all of the unknowns to the boundary surface, analogous to the Helmholtz BIE treatment of the exterior fluid domain. This can be achieved using the elastodynamic BIE which relates the displacement u and traction t on the boundary surface S (Tong and Chew 2007):

$$\frac{1}{2}u_j(\mathbf{y}) = \int_S \left[u_j(\mathbf{x})T_{ij}(\mathbf{x},\mathbf{y}) - t_j(\mathbf{x})U_{ij}(\mathbf{x},\mathbf{y}) \right] dS(\mathbf{x}) \quad (7)$$

where $\mathbf{x}$ and $\mathbf{y}$ are boundary points and U_{ij} and T_{ij} are the displacement and traction fundamental solutions (Bonnet 1999). It has been shown that the fundamental solutions for the elastodynamic BIE can be expressed in terms of the Helmholtz Green's functions and thus the FMM has been used to accelerate the solution of the

elastodynamic BIE (Fujiwara 2000, Chaillat 2008, Bonnet, Chaillat, and Semblat 2009). Equation (7) similarly does not natively include dissipation effects via viscoelasticity, but these effects can be incorporated by making the Lame parameters (which appear in U_{ij} and T_{ij}) complex valued (Chaillat 2008).

The FMBEM code being developed at CMST has recently been extended to allow coupled fluid-structure interaction problems to be modeled, where both the fluid *and* structural domains are treated with a BIE equation (Helmholtz for the fluid and elastodynamic for the solid) and both are accelerated using the FMM. A comparison of the coupled FMBEM results with those from the commercial software which uses the standard BEM for the exterior fluid domain and a standard FEM for the interior structure was intended. Unfortunately, the commercial software calculated asymmetric results for the plane wave incident on the damping plate in the plane of symmetry (which should obviously yield a symmetric solution) regardless of the frequency or BEM stabilisation technique used. Hence the initial coupled results presented from the FMBEM code have not yet been validated.

Therefore, only one set of coupled surface pressure results are shown, for the maximum 10kHz frequency where the total field is most complicated due to the shorter wavelength. The FMBEM rigid and coupled results are shown in Figure 7.
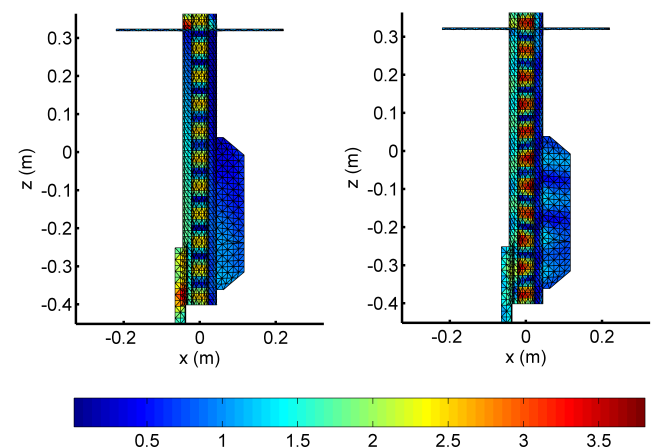
Figure 7: Comparison of the rigid (left) and coupled (right) FMBEM results for the calculated total surface pressure shown at 10kHz for a unit strength incident plane wave. The colour variation indicates the total surface pressure in Pascals.

The differences between the sets of total surface pressure results are quite interesting, particularly that the largest pressures observed on the outer surface are significantly smaller in magnitude on the coupled model, which now allows the surface to distort under the effect of the acoustic field. Also the peak pressure rings on the inner cylinder surface are higher for the coupled model and now show asymmetry with respect to the width of each peak depending on their proximity to the cylinder attachments. The coupled model was also run at 4.5kHz where it was observed that the peak pressure inside the cylinder dropped significantly to less than half of that for the rigid case. The model of the low resolution damping plate containing 8196 elements (but now 32,784 unknowns: 1 pressure and the 3 displacement components per element) was solved by the coupled

FMBEM at 10kHz in about 108 minutes, taking about 200 GMRES iterations to converge.

CONCLUSIONS

This paper has discussed the numerical modeling of a damping plate that was undertaken as part of noise modeling for using the Australian Antarctic Division's vessel the *Aurora Australis* as a launch platform for AUVs. The numerical modeling of the damping plate revealed some interesting results when comparing the calculated total surface pressure between the FMBEM code being developed at CMST and a commercial BEM software. At certain frequencies the disagreement or 'error' between the FMBEM and BEM results was quite large. Some of these errors were in part due to the small approximations introduced by using the FMBEM and it was suspected that the remainder of the errors might be caused by the 'non-uniqueness' of the exterior BEM at certain eigenfrequencies of the equivalent interior problem. However it was determined that the solutions were stable at the suspect frequencies using the standard (Burton-Miller, CHIEF) stabilisation methods and that these methods were calculating different peak pressures along the inner cylinder surface of the damping plate model. The peak pressures corresponded to the maxima and minima of the standing waves for the resonant frequencies of the tube down the middle of the structure and the largest errors observed between the models were at frequencies very close to these resonant frequencies.

The discrepancies between the calculated peak pressures for the models seems to be a result of the fact that the rigid model does not take into account energy dissipation via fluid viscosity. The structure was treated as rigid in the initial error modeling analysis when a better approximation is to treat it as elastic to allow a fully coupled fluid-structure interaction, and furthermore should involve structural damping. The FMBEM code now has the ability to model coupled fluid-structure interactions but satisfactory results from the commercial software could not be achieved for comparison with the FMBEM. Some initial coupled FMBEM results indicate that treating the structure as elastic substantially reduced the peak pressure of the standing wave at one of the resonant frequencies. Further work will involve a comparison of the coupled FMBEM and commercial BEM results followed by introducing damping in both fluid and structural domains via complex wavenumbers to see how this affects the results near the resonant frequencies.

ACKNOWLEDGEMENTS

REFERENCES

Ali, A. and C. Rajakumar (2004). *The Boundary Element Method: Applications in Sound and Vibration*. Leiden: A. A. Belkema Publishers.

Amini, S., P. J. Harris, and D. T. Wilton (1992). *Coupled Boundary and Finite Element Methods for the Solution of the Dynamic Fluid-Structure Interaction Problem*. Ed. by C. A. Brebbia and S. A. Orszag. Lecture Notes in Engineering 77. Berlin: Springer-Verlag.

Amini, S. and A. T. J. Profit (2003). "Multi-level Fast Multipole Solution of the Scattering Problem". In *Eng. Anal. Boundary Elem.* 27, pp. 547–564.

Bonnet, M. (1999). *Boundary Integral EQuation Methods for Solids and Fluids*. Wiley.

Bonnet, M., S. Chaillat, and J. F. Semblat (2009). "Multi-Level Fast Multipole BEM for 3-D Elastodynamics". In *Recent Advances in Boundary Element Methods*. Ed. by G. D. Manolis and D. Polyzos. Springer, pp. 15–27.

Brunner, D., M. Junge, and L. Gaul (2009). "A comparison of FE-BE coupling schemes for large-scale problems with fluid-structure interaction". In *Int. J. Num. Meth Engng.* 77, pp. 664–688.

Brunner, D. et al. (2010). "Comparison of the Fast Multipole Method with Hierachial Matrices for the Helmholtz-BEM". In *CMES-Comp. Model. Eng.* 58.2, pp. 131–158.

Burton, A. J. and G. F. Miller (1971). "The application of integral equation methods to the numerical solution of some exterior boundary value problems". In *Proc. Roy. Soc. Lond. A.* 323.1553, pp. 201–210.

Chaillat, S. (2008). "Fast Multipole Method for 3-D elastodynamic boundary integral equations. Application to seismic wave propagation." PhD thesis. Laboratoire de Mecanique des Solides, Ecole Polytechnique.

Chen, Z. (2005). *Finite Element Methods and Their Applications*. Berlin: Springer-Verlag.

Coifman, R., V. Rokhlin, and S. Wandzura (1993). "The Fast Multipole Metrhod for the Wave Equation: A Pedestrian Prescription". In *IEEE Antennas Propag.* 35.3, pp. 7–12.

Fischer, M. and L. Gaul (2005). "Fast BEM-FEM mortar coupling for acoustic-structure interaction". In *Int. J. Numer. Meth. Engng.* 62, pp. 1677–1690.

Fujiwara, H. (2000). "A fast multipole method for solving integral equations of three-dimensional topography and basin problems". In *Geophys. J. Int.* 140, pp. 198–210.

Gaul, L., D. Brunner, and M. Junge (2009). "Simulation of Elastic Scattering with a Coupled FMBE-FE Approach". In *Recent Advances in Boundary Element Methods*. Ed. by G. D. Manolis and D. Polyzos. Springer, pp. 131–145.

Gumerov, N. A. and R. Duraiswami (2003). "Recursions for the computation of multipole translation and rotation coefficients for the 3-D Helmholtz equation". In *SIAM J. Sci. Comput.* 25, pp. 1344–1381.

Gumerov, N. A. and R. Duraiswami (2004). *Fast Multipole Methods for the Helmholtz Equation in Three Dimensions*. Elsevier Series in Electromagnetism. Elsevier.

Gumerov, N. A. and R. Duraiswami (2007). *Fast Multipole Accelerated Boundary Element Methods for the 3D Helmholtz Equation*. Tech. rep. Perceptual Interfaces, Reality Laboratory, Department of Computer Science, and Institute for Advanced Computer Studies, University of Maryland.

Gumerov, N. A. and R. Duraiswami (2009). "A broadband fast multipole accelerated boundary element method for the 3D Helmholtz equation". In *J. Acoust. Soc. Am.* 125.1, pp. 191–205.

Hwang, W. S. (1997). "Hypersingular boundary integral equations for exterior acoustic problems". In *J. Acoust. Soc. Am.* 101.6, pp. 3336–3342.

Ihlenburg, F. (2008). "Sound in Vibrating Cabins: Physical Effects, Mathematical Description, Computational Simulation with FEM". In *Computational Aspects of Structural Acoustics and Vi-

bration. Ed. by G. Sandberg and R. Ohayon. Vol. 505. CISM Courses and Lectures. Springer.

Jensen, F. B. et al. (2000). *Computational Ocean Acoustics*. AIP Series in Modern Acoustics and Signal Processing. New York: Springer-Verlag.

Kirkup, S. M. (1998). *The Boundary Element Method in Acoustics*. Integrated Sound Software.

Li, S. and Q. Huang (2010). "An improved form of the hypersingular boundary integral equation for exterior acoustic problems". In *Eng. Anal. Boundary Elem.* 34, pp. 189–195.

Liu, Y. (2009). *Fast Multipole Boundary Element Method: Theory and Applications in Engineering*. New York: Cambridge University Press.

Liu, Y. and F. J. Rizzo (1992). "A weakly singular form of the hypersingular boundary integral equation applied to 3-D acoustic wave problems". In *Computer Methods in Applied Mechanics and Engineering* 96, pp. 271–287.

Marburg, S. (2008). "Discretization Requirements: How many Elements per Wavelength is Necessary?" In *Computational Acoustics of Noise Propagation in Fluids - Finite and Boundary Element Methods*. Ed. by S. Marburg and N. Nolte. Vol. 14. 309-332. Springer. Chap. 11.

Marburg, S. and T-W. Wu (2008). "Treating the Phenomenom of Irregular Frequencies". In *Computational Acoustics of Noise Propagation in Fluids*. Ed. by S. Marburg and B. Nolte. Berlin: Springer-Verlag. Chap. 15.

Mechel, F. P. (2008). *Formulas of Acoustics*. Ed. by C. Baumann and K. Kindler. 2nd edition. Springer.

Nishimura, N. (2002). "Fast multipole accelerated boundary integral equation methods". In *Appl. Mech. Rev.* 55.4, pp. 299–324.

Nomura, Y., I. Yamamura, and S. Inawashiro (1960). "On the Acoustic Radiation from a Flanged Circular Pipe". In *J. Phys. Soc. Jpn.* 15.3, pp. 510–517.

Reddy, J. N. (2004). *An Introduction to Nonlinear Finite Element Analysis*. New York: Oxford University Press.

Schenck, H. A. (1968). "Inproved Integral Formulation for Acoustic Radiation Problems". In *J. Acoust. Soc. Am.* 44.1, pp. 41–58.

Schneider, S. (2008). "FE/FMBE coupling to model fluid-structure interactions". In *Int. J. Numer. Meth. Engng.* 76, pp. 2137–2156.

Seybert, A. F. and T. L. Rengarajan (1987). "The use of CHIEF to obtain unique solutions for acoustic radiation using boundary integral equations". In *J. A* 81.5, pp. 1299–1306.

Silva, F. et al. (2009). "Approximation formulae for the acoustic radiation impedance of a cylindrical pipe". In *J. Sound Vib.* 322, pp. 255–263.

Tong, M. S. and W. C. Chew (2007). "Nystrom method for elastic wave scattering by three-dimensional obstacles". In *J. Comput. Phys.* 226, pp. 1845–1858.

Wrobel, L. C. (2002). *The Boundary Element Method: Applications in Thermo-Fluids and Acoustics*. Vol. 1. England: JohnWiley & Sons.

Wu, T. W. (2000). "The Helmholtz integral equation". In *Boundary Element Acoustics: Fundamentals and Computer Codes*. Ed. by T. Wu. Advances in Boundary Elements Series. Great Britain: WIT Press.

Xiao, H. and Z. Chen (2007). "Numerical experiments of preconditioned Krylov subspace methods solving the dense nonsymmetric systems arising from BEM". In *Eng. Anal. Boundary Elem.* 31, pp. 1013–1023.

Zienkiewicz, O. C. and R. L. Taylor (2000). *Finite Element Method*. 5th. Vol. 1. Elsevier.